MODELING AND SIMULATION OF HYBRID MICROGRID AND ITS COORDINATION CONTROL

PRASAD ANIPIREDDY[1], PRASAD MODDULURI[2]

[1]*Department of electrical and electronics engineering, Narayana Engineering College, Nellore,Ap,India.*

2 Asst.proffesor Department of electrical and electronics engineering, Narayana Engineering College, Nellore,Ap,India.

[1]**prasad.263@gmail.com**,[2] *prasad7040@gmail.com*

Abstract- This paper presents the modeling and simulation of hybrid microgrid and its coordination control. The microgrid concept introduces the reduction of multiple reverse conversions in an individual AC or DC grid and also facilitates connections to variable renewable AC and DC sources and loads to power systems. The interconnection of DGs to the utility/grid through power electronic converters has risen concerned about safe operation and protection of equipment's. To the customer the microgrid can be designed to meet their special requirements; such as, enhancement of local reliability, reduction of feeder losses, local voltages support, increased efficiency through use of waste heat, correction of voltage sag or uninterruptible power supply. The hybrid microgrid can operate in a grid-tied or autonomous mode.

Here photovoltaic system, wind turbine generator and battery are used for the development of microgrid. Also control mechanisms are implemented for the converters to properly coordinate the AC sub-grid to DC sub-grid. The results are obtained from the MATLAB/ SIMULINK environment.

Keywords- PV system, Wind power generation, Energy management, MPPT, DFIG, Grid control and its operation, Hybrid micro grid and power electronic converters.

I.INTRODUCTION

Power systems currently undergo considerable change in operating requirements mainly as a result of deregulation and due to an increasing amount of distributed energy resources (DER). In many cases DERs include different technologies that allow generation in small scale (microsources) and some of them take advantage of renewable energy resources (RES) such as solar, wind or hydro energy. Having microsources close to the load has the advantage of reducing transmission losses as well as preventing network congestions.

THREE PHASE ac power systems have existed for over 100 years due to their efficient transformation of ac power at different voltage levels and over long distance as well as the inherent characteristic from fossil energy driven rotating machines. Recently more renewable power conversion systems are connected in low voltage ac distribution systems as distributed generators or ac micro grids due to environmental issues caused by conventional fossil fueled power plants. On other hand, more and more dc loads such as light-emitting diode (LED) lights and electric vehicles (EVs) are connected to ac power systems to save energy and reduce CO emission.

AC micro Grids have been proposed to facilitate the connection of renewable power sources to conventional ac systems. However, dc power from photovoltaic (PV) panels or fuel cells has to be converted into ac using dc/dc boosters and dc/ac inverters in order to connect to an ac grid. In an ac grid, embedded ac/dc and dc/dc converters are required for various home and office facilities to supply different dc voltages. AC/DC/AC converters are commonly used as drives in order to control the speed of ac motors in industrial plants.

Multiple reverse conversions required in individual ac or dc grids may add additional loss to the system operation and will make the current home and office appliances more complicated.

A hybrid ac/dc microgrid is proposed in this paper to reduce processes of multiple reverse conversions in an individual ac or dc grid and to facilitate the connection of various renewable ac and dc sources and loads to power system. Since energy management, control, and operation of a hybrid grid are more complicated than those of an individual ac or dc grid, different operating modes of a hybrid

ac/dc grid have been investigated. The coordination control schemes among various converters have been proposed to harness maximum power from renewable power sources, to minimize power transfer between ac and dc networks, and to maintain the stable operation of both ac and dc grids under variable supply and demand conditions when the hybrid grid operates in both grid-tied and islanding modes. The advanced power electronics and control technologies used in this paper will make a future power grid much smarter.

There are various advantages offered by microgrids to end-consumers, utilities and society, such as: improved energy efficiency, minimized overall energy consumption, reduced greenhouse gases and pollutant emissions, improved service quality and reliability, cost efficient electricity infrastructure replacement.

II.SYTEM CONFIGURATION AND MODELING

A. Grid Configuration

Fig. 1 shows a conceptual hybrid system configuration where various ac and dc sources and loads are connected to the corresponding dc and ac networks. The ac and dc links are connected together through two transformers and two four-quadrant operating three phase converters. The ac bus of the hybrid grid is tied to the utility grid.

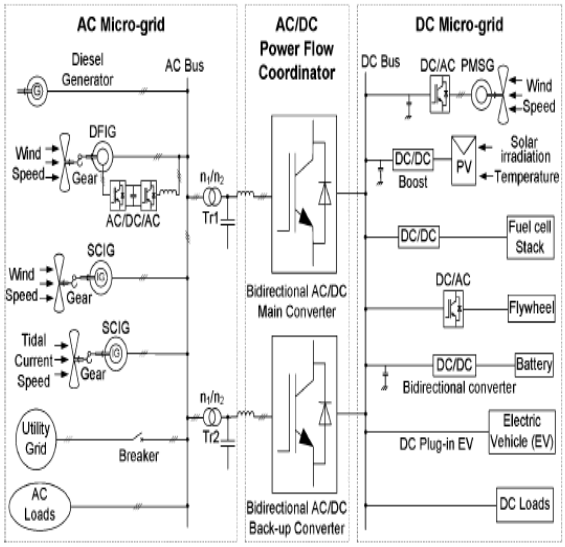

Fig.1. A Hybrid ac/dc microgrid system.

A compact hybrid grid as shown in Fig. 2 is modeled using the Simulink in the MATLAB to simulate system operations and controls. Forty kW PV arrays are connected to dc bus through a dc/dc boost converter to simulate dc sources.

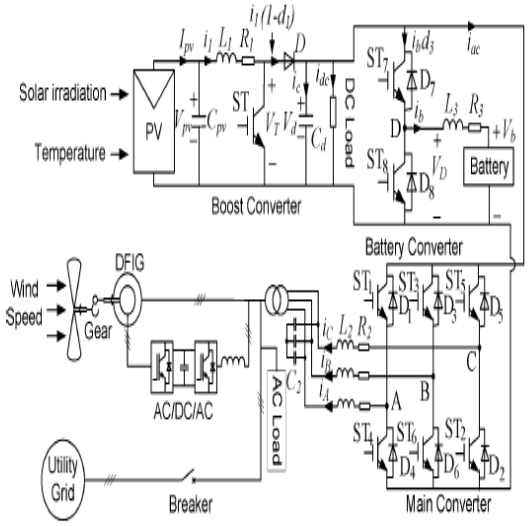

Fig.2. A compact representation of the proposed hybrid grid.

A capacitor Cpv is to suppress high frequency ripples of the PV output voltage. A 50 kW wind turbine generator (WTG) with doubly fed induction generator (DFIG) is connected to an ac bus to simulate ac sources. A 65 Ah battery as energy storage is connected to dc bus through a bidirectional dc/dc converter. Variable dc load (20 kW–40 kW) and ac load (20 kW–40 kW) are connected to dc and ac buses respectively. The rated voltages for dc and ac buses are 400 V and 400 V rms respectively. A three phase bidirectional dc/ac main converter with R-L-C filter connects the dc bus to the ac bus through an isolation transformer.

B. Grid Operation

The hybrid grid can operate in two modes. In grid-tied mode, the main converter is to provide stable dc bus voltage and required reactive power and to exchange power between the ac and dc buses. The boost converter and WTG are controlled to provide the maximum power. When the output power of the dc sources is greater than the dc loads, the converter acts as an inverter and injects power from dc to ac side. When the total power generation is less than the total load at the dc side, the converter injects power from the ac to dc side. When the total power generation is greater than the total load in the hybrid grid, it will inject power to the utility grid. Otherwise, the hybrid grid will receive power from the utility grid.

In the grid tied mode, the battery converter is not very important in system operation because power is balanced by the utility grid. In autonomous mode, the battery plays a very important role for both power balance and voltage stability. Control objectives for various converters are dispatched by energy management system. DC bus voltage is maintained stable by a battery converter or boost converter according to different operating conditions. The main converter is controlled to provide a stable and high quality ac bus voltage. Both PV and WTG can operate on maximum power point tracking (MPPT) or off-MPPT mode based on system operating requirements. Variable wind speed and solar irradiation are applied to the WTG and PV arrays respectively to simulate variation of power of ac and dc sources and test the MPPT control algorithm.

C. Modeling of Photovoltaic Panel

Fig. 3 shows the equivalent circuit of a PV panel with a load. Where, Rs is the very small series resistance and Rsh is the quite large shunt resistance. Dj is the ideal P-N diode, I*ph* expresses as the photocurrent source generated proportionally by the surface temperature and insolation. V and I represent the output voltage and output current of the solar cell, respectively.

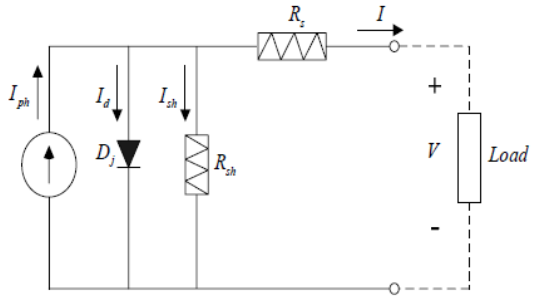

Fig. 3. Equivalent circuit of a solar cell.

The current output of the PV panel is modeled by the following three equations.

$$I_{pe} = n_p I_{ph} - n_p I_{sat} \times \left[\exp\left(\left(\frac{q}{AkT}\right)\left(\frac{V_{pv}}{n_s} + I_{pv}R_s\right)\right) - 1\right] \quad (1)$$

$$I_{ph} = (I_{sso} + K_i(T - T_r)) \cdot \frac{S}{1000} \quad (2)$$

$$I_{sat} = I_{rr} () \left(\frac{T}{T_r}\right)^3 exp\left(\left(\frac{qE_{gap}}{KA}\right) \cdot \left(\frac{1}{T_r} - \frac{1}{T}\right)\right) \quad (3)$$

All the parameters are shown in Table I:

TABLE I
PARAMETERS FOR PHOTOVOLTAIC PANEL

Symbol	Description	Value
V_{oc}	Rated open circuit voltage	403 *V*
I_{ph}	Photocurrent	
I_{sat}	Module reverse saturation current	
q	Electron charge	1.602×10^{-19} *C*
A	Ideality factor	1.50
k	Boltzman constant	1.38×10^{-23} *J/K*
R_s	Series resistance of a PV cell	
R_p	parallel resistance of a PV cell	
I_{sso}	Short-circuit current	3.27 *A*
k_i	SC current temperature coefficient	$1.7e^{-3}$
T_r	Reference temperature	301.18 *K*
I_{rr}	Reverse saturation current at T_r	$2.0793e^{-6}$ *A*
E_{gap}	Energy of the band gap for silicon	1.1*eV*
n_p	Number of cells in parallel	40
n_s	Number of cells in series	900
S	Solar radiation level	0~1000 W/m^2
T	Surface temperature of the PV	350 *K*

D. Modeling of Battery

The battery is modelled using a simple controlled voltage source in series with a constant resistance, as shown in Fig.4.

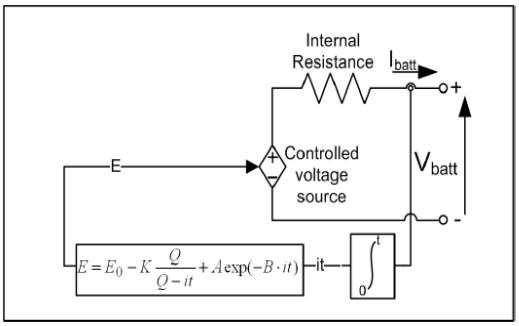

Fig.4.Non-Linear battery model

Where

$\int idt$ = actual battery charge (Ah)
A = exponential zone amplitude (V)
B = exponential zone time constant inverse $(Ah)^{-1}$
V_{batt} = battery voltage (V)
R = internal resistance (Ω)
i = battery current (A)

Two important parameters to represent state of a battery are terminal voltage Vb and state of charge (SOC) as follows.

$$V_b = V_\sigma + R_b . i_b - K\frac{Q}{Q+\int I_b\,dt} + A.exp(B\int i_b\,dt) \quad (4)$$

$$SOC = 100\left(1+\frac{\int i_b\,dt}{Q}\right) \quad (5)$$

E. Modeling of Wind Turbine Generator

Power output Pm from a WTG is determined by

$$P_m = 0.5\rho A C_p(\lambda,\beta)V_w^3 \quad (6)$$

Where ρ is air density, A is rotor swept area V_w is wind speed, $C_p(\lambda,\beta)$ and is the power coefficient, which is the function of tip speed ratio λ and pitch angle β.

The mathematical models of a DFIG are essential requirements for its control system. The voltage equations of an induction motor in a rotating d-q coordinate are as follows:

$$\begin{bmatrix} u_{ds} \\ u_{qs} \\ u_{dr} \\ u_{qr} \end{bmatrix} = \begin{bmatrix} -R_s & 0 & 0 & 0 \\ 0 & -R_s & 0 & 0 \\ 0 & 0 & R_r & 0 \\ 0 & 0 & 0 & R_r \end{bmatrix} \begin{bmatrix} i_{ds} \\ i_{qs} \\ i_{dr} \\ i_{qr} \end{bmatrix} + p\begin{bmatrix} \lambda_{ds} \\ \lambda_{qs} \\ \lambda_{dr} \\ \lambda_{qr} \end{bmatrix} + \begin{bmatrix} -\omega_1\lambda_{qs} \\ \omega_1\lambda_{ds} \\ -\omega_2\lambda_{qr} \\ \omega_2\lambda_{dr} \end{bmatrix} \quad (7)$$

$$\begin{bmatrix} \lambda_{ds} \\ \lambda_{qs} \\ \lambda_{dr} \\ \lambda_{qr} \end{bmatrix} = \begin{bmatrix} -L_s & 0 & L_m & 0 \\ 0 & -L_s & 0 & L_m \\ -L_m & 0 & L_r & 0 \\ 0 & -L_m & 0 & L_r \end{bmatrix} \begin{bmatrix} i_{ds} \\ i_{qs} \\ i_{dr} \\ i_{qr} \end{bmatrix}. \quad (8)$$

The dynamic equations of the DFIG are given by

$$\frac{J}{n_p}\frac{dw_r}{dt} = T_m - T_{em} \quad (9)$$

$$T_{em} = n_p L_m\left(i_{qs}i_{dr} - i_{ds}i_{qr}\right) \quad (10)$$

Where the subscripts d, q, s and denote d-axis, q-axis, stator, and rotor respectively, L represents the inductance, λ is the flux linkage, u and i represent voltage and current respectively, ω_1 and ω_2 are the angular synchronous speed and slip speed respectively, $\omega_2 = \omega_1 - \omega_r$, T_m is the mechanical torque, T_{em} is the electromagnetic torque.

III.COORDINATION CONTROL OF THE CONVERTERS

There are five types of converters in the hybrid grid. Those converters have to be coordinately controlled with the utility grid to supply an uninterrupted, high efficiency, and high quality power to variable dc and ac loads under variable solar irradiation and wind speed when the hybrid grid operates in both isolated and grid tied modes. The control algorithms for those converters are presented in this section.

The combined time average model for the booster and main converter is shown in fig.4.

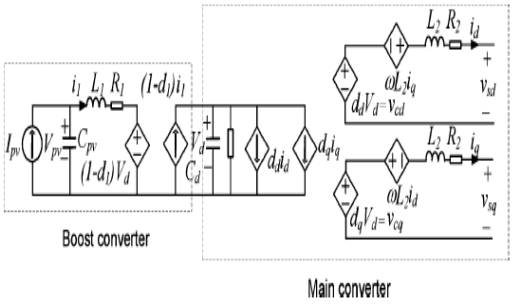

Fig.4. Time average model for the booster and main converter

The DTC control scheme for the rotor side converter and control mode diagram for the isolated hybrid grid is shown in fig.5 and fig.6

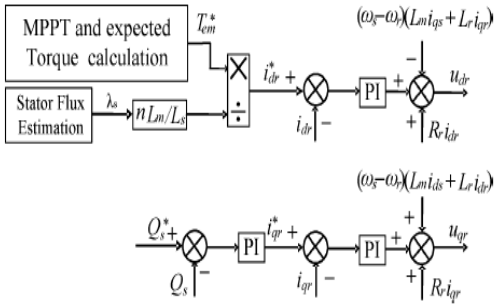

Fig.5. DTC control scheme for the rotor side converter

Two level coordination controls are used to maintain system stable operation. At the system level, operation modes of the individual converters are determined by the energy management system (EMS) based on the system net power and the energy constraints and the charging/discharging rate of battery.

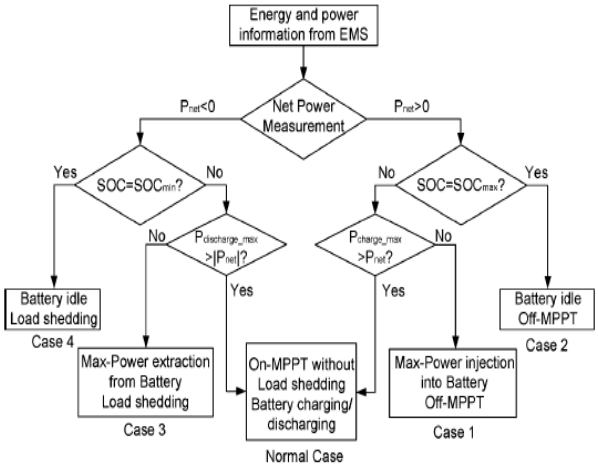

Fig.6. control mode diagram for the isolated hybrid grid

For both Grid connected and Isolated mode of operations the power flow equations are required. Power flow equations at the dc and ac links are as follows

$$P_{pv} + P_{ac} = P_{dcl} + P_b \quad (11)$$

$$P_s = P_w - P_{acL} - P_{ac} \quad (12)$$

Where real power P_{pv} and P_w are produced by PV and WTG respectively. P_{acL}, P_{dcL} are real power loads connected to ac and dc buses respectively. P_b is power injection to battery and P_s power injection from the hybrid grid to the utility.

Powers under various load and supply conditions should be balanced as follows:

$$P_{pv} + P_a = P_{acL} + P_{dcL} + P_{loss} + P_b \quad (13)$$

Where P_{loss} is the total grid loss.

IV.SIMULATION RESULTS

The operations of the hybrid grid under various source and load conditions are simulated to verify the proposed control algorithms. The parameters of components for the hybrid grid are listed in Table II.

TABLE II
Component parameters for the hybrid grid

Symbol	Description	Value
C_{pv}	Capacitor across the solar panel	*110uF*
L_1	Inductor for the boost converter	*2.5mH*
C_d	Capacitor across the dc-link	*4700uF*
L_2	Filtering inductor for the inverter	*0.43mH*
R_2	Equivalent resistance of the inverter	*0.3ohm*
C_2	Filtering capacitor for the inverter	*60uF*
L_3	Inductor for the Battery converter	*3mH*
R_3	Resistance of L3	*0.1ohm*
f	Frequency of the AC grid	*60Hz*
f_s	Switching frequency of power converters	*10kHz*
V_d	Rated DC bus voltage	*400V*
V_{ll_rms}	Rated AC bus line voltage *(rms value)*	*400V*
n_1/n_2	Ratio of the transformer	*2:1*

(1) Solar panel

The solar irradiation level is set as 400 $\frac{\omega}{m^2}$ from 0.0 s to 0.1 s, increases linearly to 1000 $\frac{\omega}{m^2}$ from 0.1 s to 0.2 s, keeps constant until 0.3 s, decreases to W/m from 0.3 s to 0.4 s and keeps that value until the final time 0.5 s. The initial voltage for the P&O is set at 250 V. It can be seen that the P&O is continuously tracing the optimal voltage from 0 to 0.2 s. The algorithm only finds the optimal voltage at 0.2 s due to the slow tracing speed. The algorithm is searching the new optimal voltage from 0.3 s and finds the optimal voltage at 0.48 s. It can be seen that the basic algorithm can correctly follow the change of solar irradiation but needs some time to search the optimal voltage. The improved P&O methods with fast tracing speed should be used in the PV sites with fast variation of solar irradiation.

The terminal voltage and PV out power versus solar irradiation simulation results are shown in fig.7. and fig.8.

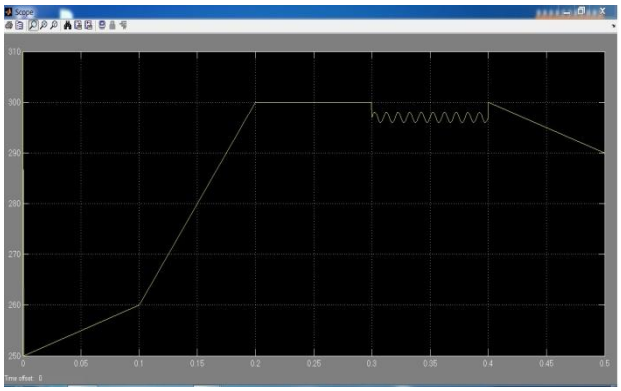

Fig.7.Teminal voltage of solar panel

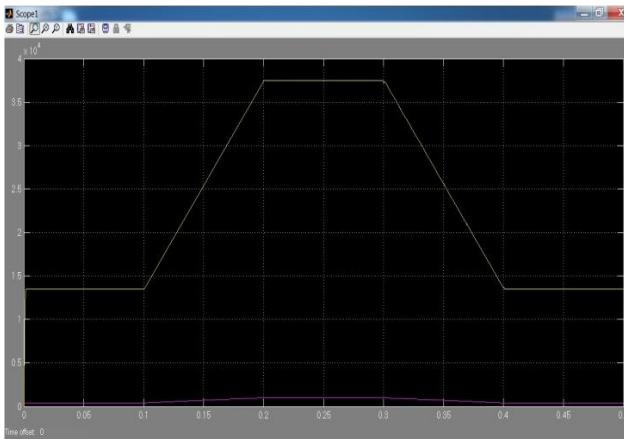

Fig.8.PV output power versus solar irradiation

The above fig.8.shows the curves of the solar radiation (radiation level times 30 for comparison) and the output power of the PV panel. The output power varies from 13.5 kW to 37.5 kW, which closely follows the solar irradiation when the ambient temperature is fixed.

(2) DFIG

The dynamic responses at the ac side of the main converter when the ac load increases from 20 kW to 40 kW at 0.3 s with a fixed wind speed 12 m/s. It is shown clearly that the ac grid injects power to the dc grid before 0.3 s and receives power from the dc grid after 0.3 s. The output power of the DFIG and AC side voltage versus current (voltage times 1/3 for comparison).

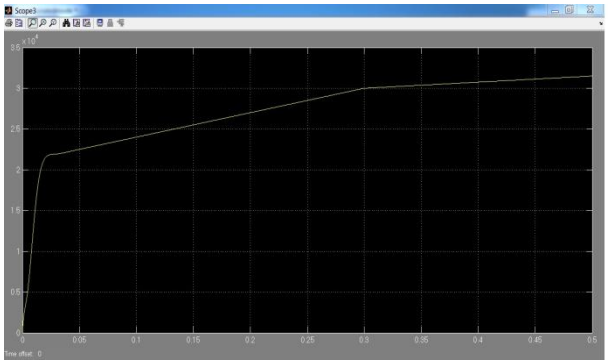

Fig.9.Output power of the DFIG

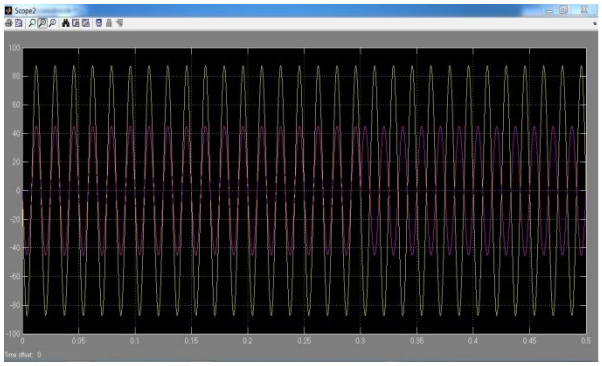

Fig.10.AC side voltage versus current

(3)Battery

The nominal voltage and rated capacity of the battery are selected as 200 V and 65 Ah respectively. Fig. 11 shows the current and SOC of the battery. Fig. 12 shows the voltage of the battery. The total power generated is greater than the total load before 0.3s and less than the total load after 0.3s. It can be seen from Fig. 11 that the battery operates in charging mode before 0.3s because of the positive current and discharging mode after 0.3s due to the negative current. The SOC increases and decreases before and after 0.3 s respectively. Fig. 12 shows that the voltage drops at 0.3s and recovers to 400V quickly.

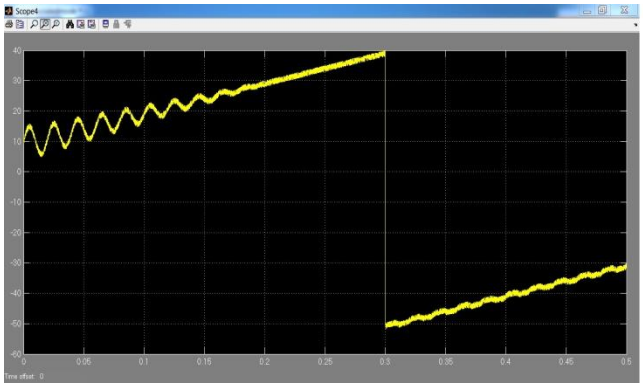

Fig.11. Battery charging current

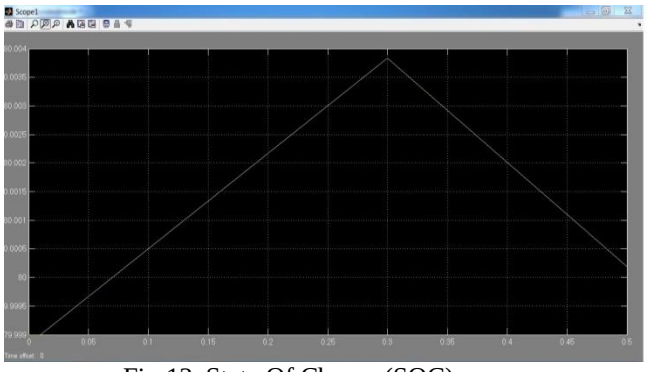

Fig.12. State Of Charge (SOC)

The DC bus voltage transient response is shown in fig.13

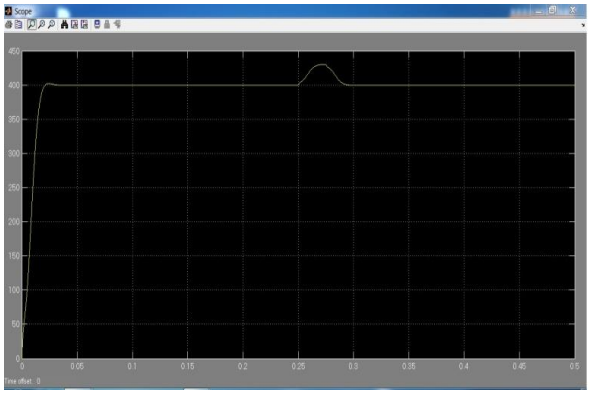

Fig.13. DC bus voltage transient response

V CONCLUSION

A hybrid ac/dc micro grid is proposed and comprehensively studied in this paper. The models and coordination control schemes are proposed for the all the converters to maintain stable system operation under various load and resource conditions. The coordinated control strategies are verified by MATLAB/Simulink. Various control methods have been incorporated to harness the maximum power from dc and ac sources and to coordinate the power exchange between dc and ac grid. Different resource conditions and load capacities are tested to validate the control methods. The simulation results show that the hybrid grid can operate stably in the grid-tied or isolated mode. Stable ac and dc bus voltage can be guaranteed when the operating conditions or load capacities change in the two modes. The power is smoothly transferred when load condition changes.

Although the hybrid grid can reduce the processes of dc/ac and ac/dc conversions in an individual ac or dc grid, there are many practical problems for implementing the hybrid grid based on the current ac dominated infrastructure. The total system efficiency depends on the reduction of conversion losses and the increase for an extra dc link. It is also difficult for companies to redesign their home and office products without the embedded ac/dc rectifiers although it is theoretically possible. Therefore, the hybrid grids may be implemented when some small customers want to install their own PV systems on the roofs and are willing to use LED lighting systems and EV charging systems. The hybrid grid may also be feasible for some small isolated industrial plants with both PV system and wind turbine generator as the major power supply.

REFERENCES

[1] R. H. Lasseter, “Micro Grids,” in Proc. IEEE Power Eng. Soc. Winter Meet., Jan. 2002, vol. 1, pp. 305–308.

[2] Y. Zoka, H. Sasaki, N. Yorino, K. Kawahara, and C. C. Liu, “An interaction problem of distributed generators installed in a Micro Grid,” in Proc. IEEE Elect. Utility Deregulation, Restructuring. Power Technol., Apr. 2004, vol. 2, pp. 795–799.

[3] R. H. Lasseter and P. Paigi, “Micro grid: A conceptual solution,” in Proc. IEEE 35th PESC, Jun. 2004, vol. 6, pp. 4285–4290.

[4] C. K. Sao and P. W. Lehn, “Control and power management of converter fed Micro Grids,” IEEE Trans. Power Syst., vol. 23, no. 3, pp. 1088–1098, Aug. 2008.

[5] T. Logenthiran, D. Srinivasan, and D.Wong, “Multi-agent coordination for DER in Micro Grid,” in Proc. IEEE Int. Conf. Sustainable Energy Technol., Nov. 2008, pp. 77–82.

[6] M. E. Baran and N. R. Mahajan, “DC distribution for industrial systems: Opportunities and challenges,” IEEE Trans. Ind. Appl., vol. 39, no. 6, pp. 1596–1601, Nov. 2003.

[7] Y. Ito, Z.Yang, and H. Akagi, “DC micro-grid based distribution power generation system,” in Proc. IEEE Int. Power Electron. Motion Control Conf., Aug. 2004, vol. 3, pp. 1740–1745.

[8] A. Sannino, G. Postiglione, and M. H. J. Bollen, “Feasibility of a DC network for commercial facilities,” IEEE Trans. Ind. Appl., vol. 39, no. 5, pp. 1409–1507, Sep. 2003.

[9] D. J. Hammerstrom, “AC versus DC distribution systems-did we get it right?,” in Proc. IEEE Power Eng. Soc. Gen. Meet., Jun. 2007, pp. 1–5.

[10] D. Salomonsson and A. Sannino, “Low-voltage DC distribution system for commercial power systems with sensitive electronic loads,” IEEE Trans. Power Del., vol. 22, no. 3, pp. 1620–1627, Jul. 2007.

[11] M. E. Ropp and S. Gonzalez, “Development of a MATLAB/Simulink model of a single-phase grid-connected photovoltaic system,” IEEE Trans. Energy Conv., vol. 24, no. 1, pp. 195–202, Mar. 2009.

[12] K. H. Chao, C. J. Li, and S. H. Ho, “Modeling and fault simulation of photovoltaic generation systems using circuit-based model,” in Proc. IEEE Int. Conf. Sustainable Energy Technol., Nov. 2008, pp. 290–294.

[13] O. Tremblay, L. A. Dessaint, and A. I. Dekkiche, “A generic battery model for the dynamic simulation of hybrid electric vehicles,” in Proc. IEEE Veh. Power Propulsion Conf. (VPPC 2007), pp. 284–289.

[14] D. W. Zhi and L. Xu, "Direct power control of DFIG with constant switching frequency and improved transient performance," IEEE Trans. Energy Conv., vol. 22, no. 1, pp. 110–118, Mar. 2007.
[15] L. Bo and M. Shahidehpour, "Short-term scheduling of battery in a grid-connected PV/battery system," IEEE Trans. Power Syst., vol. 20, no. 2, pp. 1053–1061, May 2005.

AUTHOR DETAILS

Prasad Anipireddy recived the B.Tech degree from Audisankara College of Engg & Tech,Gudur, Nellore(dt). Present he is perceive M.Tech from Narayana Engineering College, Nellore. His current research interests are power systems and solar energies.

Prasad Modduluri recived the Master degree in electrical power engineering from JNTU Anantapuram. B.Tech degree from G.Pullareddy Engineering College Kurnool in Electrical and electronics engineering branch . He had 5 years of experience in teaching field.He had published many papers in power system applications. Present he is interested in online monitoring of power system stability.